Health Biotechnology and Biopharma (2023), 7(4): 1-23

Original Research Article

Comparison of methyl isoeugenol and methyl eugenol as renewable starting reagents for the synthesis of thiourea compounds for *anti-Plasmodium falciparum*

Warsito Warsito [1,*], Elvina Dhiaul Iftitah[1] , Nashi Widodo [2], Nuryamin Kazal [1], Lucy Arianie [1,*]
[1]Chemistry Department, Faculty of Science, Universitas Brawijaya, Malang, Indonesia
[2]Biology Department, Faculty of Science, Universitas Brawijaya, Malang, Indonesia
***Corresponding authors:** Warsito Warsito and Lucy Arianie, Chemistry Department, Faculty of Science, Universitas Brawijaya, Malang, Indonesia. E-mail: lucy.brawijaya@gmail.com; warsitoub@ub.ac.id*

DOI: 10.22034/HBB.2024.01

Received: November 8, 2023; **Accepted:** December 6, 2023

ABSTRACT

Several thiourea derivative compounds have been used as inhibitors of *Plasmodium falciparum* via the plasmepsin inhibition pathway. The thiourea derivative (compound 3) namely 1-{1-(3,4-dimethoxyphenyl)-4.6-bis[(3,4-dimethoxyphenyl)methyl]heptane-2-yl]-3-{[(2E)-3-phenylprop-2-en-1-ylium-1-yl]amino}thiourea was synthesized using the one-pot synthesis method by comparing the renewable starting reagents Methyl Isoeugenol (MIE) and Methyl Eugenol (ME). Observation using FTIR and LCMS-MS was shown that ME is more representative as a precursor. Compound (3) was synthesized using ME isothiocyanate compound (2), hydrazine, and cinnamaldehyde at 70 °C for 5 h, yielding 0.2769 g (22.47 %), and the molecular ion is 740 (98 % area). *In vitro* bioactivity tests against *Plasmodium falciparum* 3D7 of compound (3) resulted in IC_{50}=10.19 ppm. Molecular docking of ligand (3) gave an insight that the compound (3) was a promising *anti-Plasmodium falciparum* compound.

***Keywords*:** Methyl isoeugenol, methyl eugenol, thiourea derivative, *Plasmodium falciparum*

INTRODUCTION

Methyl isoeugenol (Figure 1a) is the main component in the *Pimenta pseudocaryophyllus* plant [1,2]; *Veronica austriaca ssp. jacquinii (Baumg.) Eb. Fisch* [3]; *Daucus carota subsp. Maritimus*, *Daucus carota subsp. Hispidus*, and *Daucus carota subsp. Carota* [4]. Methyl isoeugenol was reported as a fiber dye,

anxiolytic, and antidepressant [1,5]. Methyl isoeugenol acts as a precursor compound [6–8]. Methyl isoeugenol has been reported as an active agent against *Aedes aegypti* larvae [9] and nematicidal [10]. Methyl isoeugenol is a more active attractant for the fruit fly *Bactrocera xanthodes (Broun)* (Dacinae) compared to methyl eugenol [11].

Methyl eugenol (1,2-dimethoxy-4-(prop-2-en-1-yl)benzene) is a compound that resembles methyl isoeugenol (1,2-dimethoxy-4-(prop-1-en-1-yl) benzene). The difference between Methyl Eugenol (ME) and Methyl Isoeugenol (MIE) lies only in the position of the double bond in the propenoid group; methyl isoeugenol has a double bond position at C2 and C3, while methyl eugenol has a double bond position at C1 and C2 (Figure 1b). Methyl isoeugenol and methyl eugenol can be derived from eugenol methylation. Eugenol is a major component in clove *Syzygium aromaticum, Ocimum basilicum, Glycine max (L.) Merr., Croton zehntneri Pax et Hoffm,* dan *Laurus nobilis L.* [12–14]. Methyl eugenol was reported as a fish anesthetic compound [15]. ME is an essential antioxidant, anti-inflammatory, anti-bacterial, anti-fungal, and attractant [16–18]. ME was a precursor in synthesizing bioactive compounds [19,20].

Many active compounds for *P. falciparum* inhibitors have urea or thiourea character, for instance, compounds were presented in Figure 1g and Figure 1h. The nitrogen and sulfur atoms in thiourea and urea predictively play a vital role in the bioactivity of the active compounds [21–23]. The precursor potencies of MIE and ME for the synthesis of thiourea derivative as *anti-Plasmodium falciparum* compounds are not yet known, and motivated to carry out this research. Malaria caused by *P. falciparum* is the most fatal infectious disease and faces drug resistance problems, making the new drug discovery continue. One focus of the drug *Plasmodium falciparum* target is plasmepsin (aspartic protease), which is important in the survival and spread of the parasite. There are ten plasmepsins in *Plasmodium falciparum*, namely PfPMI, PfPMII, PfPMIV, PfPMV, PfPMVI-X, and Histo-Aspartic Protease (HAP) [24]. PMI-IV and HAP are found in food/digestive vacuoles and play a role in Hb catabolism. This intra-erythrocytic stage is critical because the survival of the parasite depends on the consumption of host hemoglobin (Hb) in the food vacuole as the primary

amino acid source for parasite growth and maturation [25,26]. Meanwhile, PMX plays a role in therapeutic intervention as a maturase for rhoptry and microneme proteins [27–29]. Plasmepsin I and Plasmepsin X have inhibitors in the form of high molecular weight compounds and contain N, S, and urea groups.

This research aims to: 1. Conversion of MIE and ME as MIE-Isothiocyanate (1) and ME-Isothiocyanate (2); 2. Comparative analysis of synthesis products (1) and (2) using Thin Layer Chromatography (TLC), Fourier Transform Infrared (FTIR), and Liquid Chromatography-Mass Spectrometry tandem Mass Spectrometry (LCMS-MS); 3. Synthesis of thiourea derivative compound (compound 3) using one potential precursor; 4. Analysis of compound (3) using TLC, FTIR, LCMS-MS, and in vitro *P. falciparum* test; 5. Molecular docking and interaction (2D and 3D) analysis of compound (3) via *Plasmodium falciparum* Plasmepsin I (PfPMI) and *Plasmodium falciparum* Plasmepsin X (PfPMX) inhibitions.

MATERIALS AND METHODS

Methyl isoeugenol and methyl eugenol were derived from clove oil. Potassium thiocyanate (KSCN), potassium hydrogen sulfate ($KHSO_4$), chloroform, ethanol, n-hexane, ethyl acetate, sodium bicarbonate, hydrazine, cinnamaldehyde, hydrochloric acid (HCl), nitrogen gas, Thin Layer Chromatography (TLC) GF_{254} plate and supporting solvents with pro-analysis grade.

Synthesis of compound (1) and compound (2)

Compounds (1) and (2) were synthesized by using the ratio of MIE: HSCN = 1:20 (mmol) at room temperature for 24 hours. HSCN was produced by referring to modified procedures [30,31]. After 24 hours of reaction time, the orange powder was filtered, dried by nitrogen gas flow, and put in a vial. The same above procedure was applied to the ME. All the steps were done triplo. Orange-colored solid products from the synthesis process were analyzed using the TLC method. Wavenumber between 500–4000 cm^{-1} in Fourier Transform Infrared Shimadzu instrument was used to diagnose functional groups in all synthesized compounds by KBr pellet. Compounds (1) and (2) were identified by Liquid Chromatography-Mass Spectrometry tandem Mass Spectrometry (LCMS-MS) triple quadrupole 8060 Shimadzu at λ = 290 nm. One optimum

product was obtained for the synthesis precursor of the thiourea derivative.

Synthesis of compound (3)

The compound (3) was synthesized by modified one-pot methods [32–37]. Firstly, 2.86 mmol of compound (2) dissolved in ethanol. Synthesis was carried out by adding 2.86 mmol of hydrazine into a reaction flask containing 2.86 mmol of crude compound (2). The mixture was stirred at 70 °C for 5 hours. Then, without the separation process, the reaction mixture was added by 2.86 mmol of cinnamaldehyde and 5 ml of 10 % HCl. The reaction was continued for 2 hours. The yellow-colored solid phase was purified by recrystallization using hot ethanol and then analyzed using TLC, FTIR, dissolution, and melting point. Compound (3) was identified by the LCMS-MS XEVO-G2SQTOF (Waters) instrument.

The culture of Plasmodium falciparum and in vitro bioactivity test

The bioactivity of compound (3) against *Plasmodium falciparum* 3D7 (chloroquine-sensitive) was observed by in vitro assay using the Giemsa stained slide method [30,38,39]. *Plasmodium falciparum* was cultured by using the Trager and Jensen methods. The parasites were grown in fresh erythrocytes with 5 % hematocrit, 25 mM Hepes Buffer, 50 µg/ml hypoxanthine, 2 mg/ml $NaHCO_3$, and 10 µg/ml gentamycin, then incubated at 37 °C. Giemsa's stained method was used for analyzing infected erythrocytes.

The anti-Plasmodium was tested by the Giemsa stained slide procedure. Ten mg of compound (3) was diluted in 1 ml DMSO and added by RPMI-1640 medium to make serial concentration at 0.01, 0.1, 1.0, 10, and 100 µg/ml and placed in 24 well plates. Observation was done until 48 hours at the well plates after adding 500 µl parasite culture (incubated at 37 °C). The percentage of parasitemia was counted by microscope for infected erythrocytes per 1000 total erythrocytes. The growth inhibition (%) was calculated by using this equation:

Growth inhibition = 100 % - $(\frac{Xe}{Xk} \times 100\%)$

Xe=the average parasitemia of the experimental group.

Xk=the average parasitemia of negative control.

The IC_{50} values were determined by four parameters logistic curve to the dose-response data using GraphPad Prism 7.0 software.

Molecular docking

MarvinSketch was re-downloaded in October 2023 to draw the compound (3) structure. Chloroquine's structure was downloaded from *http://www.chemspider.com* and used as a co-drug ligand. *Plasmodium falciparum* plasmepsin I (PfPMI) and *Plasmodium falciparum* plasmepsin X (PfPMX) with PDB code 3QS1 chain A and 8DSR chain B, respectively, were used as receptors. Chimera optimized the structures of all receptors, chloroquine, and compound (3). Macromolecule optimization was carried out by dockprep, adding hydrogen and the Amber ff14SB AM1-BCC charge. Ligand optimization was carried out by adding hydrogen atoms and Gesteiger charges. Structure's compound (2) was also prepared for comparison. Re-docking using the native ligands was done for docking calibration.

Specific molecular docking was carried out using the PyRx-integrated Autodock Vina. The compound's molecular energy was minimized, and molecules were converted into ligands. Grid box for 3QS1 chain A and ligand was set at size x = 33.30, y = 29.59, z = 35.23. The grid box was centered at x = 26.29 Å; y = -13.10 Å, z = 5.52 Å. Whereas the grid box for specific docking of 8DSR chain B and ligands was conditioned at x = 10.01, y = 17.50, z = 19.81 in dimensions of x = -24.22 Å, y = -1.16 Å, z = 14.12 Å. The best affinities energy of complex receptor and ligand were chosen at root mean square deviation (rmsd) < 2.0. The molecular interactions (2D and 3D) inside the receptor and ligand complex were analyzed by Discovery Studio 2019 Client [40–42].

RESULTS

The reaction of MIE and thiocyanic acid at room temperature for 24 hours produces an orange solid. An orange-colored product was also formed during the reaction of ME and thiocyanic acid in different reflux apparatuses [30,31]. Preliminary TLC data shows that MIE produces a retention factor (Rf) of 0.875 while ME has two spots with Rf of 0.675 and 0.750, which are predicted as isomers of the ME compound. TLC data on compound (1) and compound (2) shows that there are new spots, including at Rf 0.40, 0.45, and 0.55 which indicates that the synthesis products are crude with several new compounds that have been formed. Elution was done by eluent n-hexane: ethyl acetate =1:1(v/v). The weight of compound

(1) was yielded 0.0277 g, and compound (2) 0.1331 g (yield 25.56 %).

The solubility test for compounds (1) and (2) was carried out in two types of solvent (DMSO and water) by adding drops of 2 ml solvent to 2.0 mg of sample in a test tube. Solubility data shows that both synthesized compounds dissolve completely in DMSO, not dissolved in water for compound (1) and partially dissolved in water for compound (2). FTIR analysis shows isothiocyanate absorption at wavenumbers 2061 cm^{-1} and 2049 cm^{-1} for compounds (1) and (2), respectively. However, the solid compound (1) shows thiocyanate absorption at around 2157 cm^{-1} which makes a deep prediction that the reaction of MIE and thiocyanic acid produces a crude thiocyanate solid compound. Melting point (Mp) analysis shows that compounds (1) and (2) have Mp 158-162 °C and 214-216 °C, respectively, which indicates that the two precursors product are crudes. LCMS-MS analysis further confirms several compounds inside the compound (2) viz fractions of ME polymerization and ME isothiocyanate products.

The LCMS-MS spectrum of compounds (1) and (2) shows that the largest areas are methyl eugenol and methyl isoeugenol polymerization. It can be understood because the isothiocyanate group is unstable and could be released during the heating process of the instrument. The conversion of methyl eugenol to ME isothiocyanate derivatives is predictively occurs by polymerization of methyl eugenol molecules, and then synthesis of compound (1) is also predicted to produce a polymer compound of MIE [30,31]. Compounds (1) and (2) each have 415.05 and 416.45 molecular ions with an area of 3.73 % and 10.59 % respectively. Since the thiourea synthesis should be arranged in the isothiocyanate pathway [34], then compound (2) was chosen as a further precursor for the synthesis of thiourea derivative compound (3). Although too premature to make compound names, the proposed scientific name for compound (1) is 4,4'-(2-methyl-4-thiocyanatopentane-1,5-diyl)bis(1,2-dimethoxybenzene) by ChemDraw or {[1-(3,4-dimethoxyphenyl)-4-[(3,4-dimethoxyphenyl)methyl]pentan-2-yl]sulfanyl}carbonitrile as a preferred IUPAC name by MarvinSketch. Whereas for compound (2) is 4,4'-(2-isothiocyanato-4-methylpentane-1,5-diyl) bis(1,2-dimethoxybenzene) named by ChemDraw or 4-[5-(3,4-dimethoxyphenyl)-2-isothiocyanato-4-methylpentyl]-1,2-

dimethoxybenzene as a preferred IUPAC name by MarvinSketch.

Compound (3) was synthesized from compound (2) using a one-pot reaction method. This kind was reported as more efficient because it does not go through the stages of thiosemicarbazide compounds forming [30,33]. The resulting compound (3) was a light brown solid phase (0.2769 g, yield 22.47 %). The Rf of compounds (2) and (3) reached 0.175 and 0.775, respectively, identified using n-hexane: ethyl acetate =3:1 (v/v) as eluent.

The infrared spectrum of compounds (2) and (3) was laid in Table 1. Comparing these compounds shows that compound (3) has absorptions at wavenumbers around 3200 – 3500 cm^{-1}, which were predicted for free -NH absorption. Vibrations of C-N and C=N were very difficult owing to their probability of mixing with several bands. In the present compound, the wavenumber 1515 cm^{-1} was predicted as C=N absorption from thiourea [43,44]. The new compound formation was also supported by the loss of wavenumber absorption at 2049 cm^{-1}, indicating that the double bond C-isothiocyanate was changed into C-N single bonds.

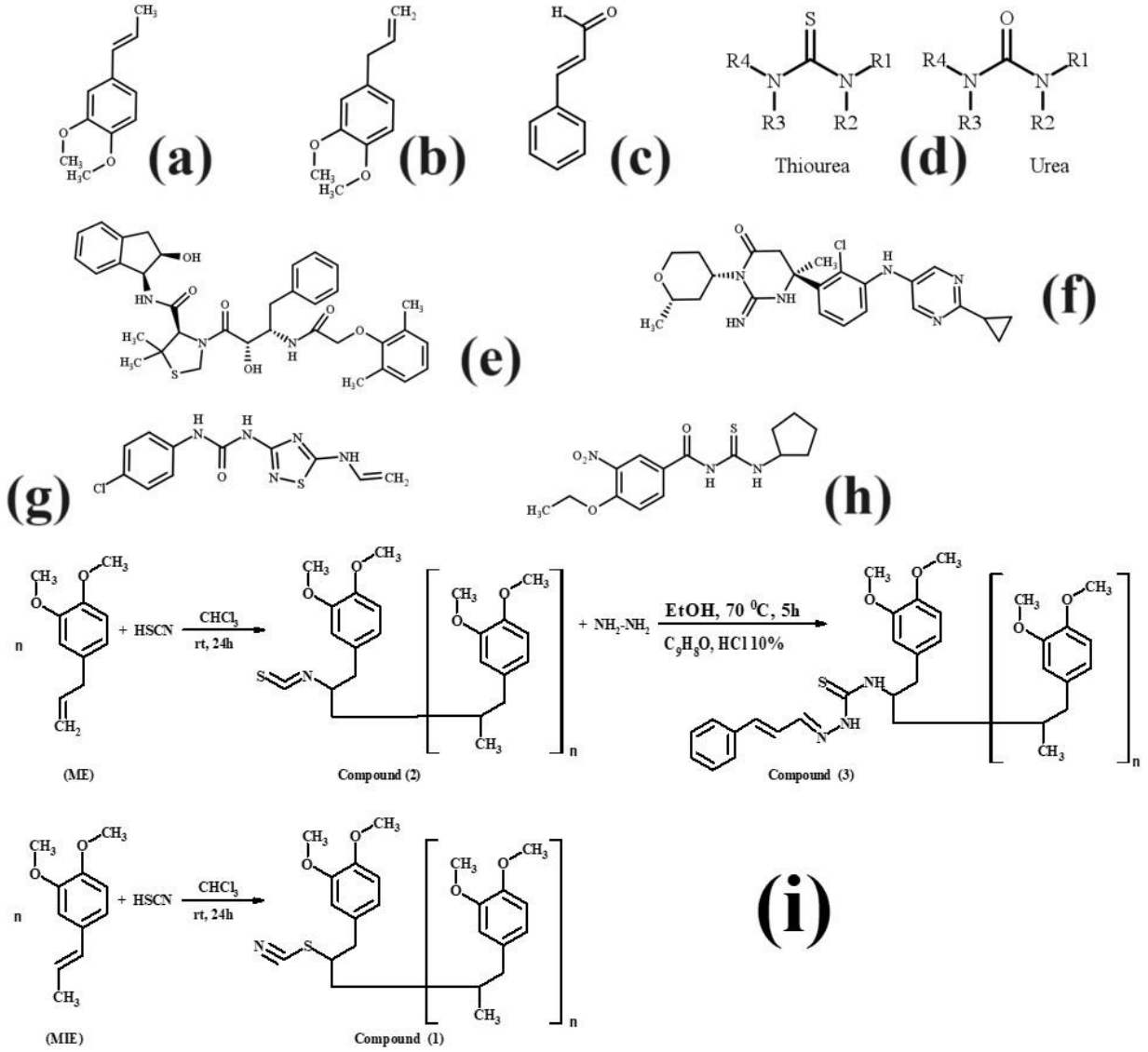

Figure 1. Structure of (a). MIE, (b). ME, (c). cinnamaldehyde, (d). thiourea, urea, (e) – (h). inhibitors of PfPMII and PfPMX [22,23,28,49], and (i). the proposed reaction of compound (3).

Table 1. Specific wavenumber profile in MIE, ME, compounds (1), (2), and (3)

Bond type	Wavenumber (cm^{-1}) prediction of compounds:				
	MIE	**ME**	**(1)**	**(2)**	**(3)**
C – H (aryl)	2840 - 3100	2900 - 3150	2900 - 3150	2900 - 3100	2900 - 3150
C-H (aliphatic)	962	2940 - 2915	2930	2923	2943
=C-H (Ar)	3083, 854, 763	3083, 854, 763	3170	3163	3323 - 3488
C=C (Ar)	1591, 1514, 1464	1587, 1507, 1467	1511	1511	1515
C=C (vynil)	960-900, 1637	915, 1597	-	-	-
C-O-C (ether)	1020, 1250	1235 – 1195	1020	1018	1169
C- H (methyl)	1375	-	1300	1300	1300
CH_2	-	1464 - 1424	1460	1463	1500
C=S	-	-	750	753	759
C=N (imino)	-	-	1600	1614	1515
-N=C=S	-	-	2061*	2049	-
-S-C=N	-	-	2157*	-	-
N-H (amine)	-	-	-	-	3400
C-N (amine)	-	-	-	-	1269

Molecular mass analysis of compound (3) was performed using LCMS-MS, producing a spectrum with several compound areas. One peak abundance (98 %) was found at 18.09 minutes of retention time with parent ion at 740 (Figure 2). The LCMS-MS spectra indicate that compound (3) is a crude compound. This crude compound prediction correlates with the broad melting point of compound (3) between 157 °C and 167 °C. The proposed structure of methyl eugenol cinnamaldehyde thiourea (MW=739) is presented in Figure 2 namely (E)-N-(4-(3,4-dimethoxybenzyl)-1,7-bis(3,4-dimethoxyphenyl)-6-methylheptan-2-yl)-2-((E)-3-phenylallylidene)hydrazine-1-carbothioamide (ChemDraw) or 1-[1-(3,4-dimethoxyphenyl)-4,6-bis[(3,4-dimethoxyphenyl)methyl]heptane-2-yl]-3-[(E)-[(2E)-3-phenylprop-2-en-1-yliden]amino]thiourea (preferred IUPAC name by MarvinSketch). Synthetic thiourea compounds tend to have high

molecular masses because the thiourea framework has two substituent sites. However, despite having a high molecular mass, many thiourea derivative compounds show good therapeutic and biological activity as drug candidates [45–48].

Compound (2) is predicted as a methyl eugenol isothiocyanate derivative that contains 2 (two) methyl eugenol molecules. The weak bond in these two ME molecules allows protonation and the formation of the thiourea derivative compound (3) which has 3 methyl eugenol molecules. It can be assumed that 3 moles of compound (2) produce 2 moles of compound (3). In the LCMS-MS spectrum of compound (3), the molecular ion m/z 562 was detected as the suspected derivative of compound (3) which contains two ME molecules. However, the highest percent retention was compound (3) with MW 739 and m/z 740.

In vitro assay of *P. falciparum* resulted in IC_{50} of compound (3) = 10.19 ppm, which means compound (3) is a promising active compound against the protozoan *Plasmodium falciparum*. This refers to the basic criteria of IC_{50} by WHO that antiparasitic compounds can be grouped into four categories, namely not active if IC_{50}>50 μg/ml, moderately active at 15 μg/ml<IC_{50}≤50 μg/ml, active at 5 μg/ml<IC_{50}≤15 μg/ml and very active at IC_{50}≤5 μg/ml [38].

Molecular docking analysis has used a macromolecule with PDB code 3QS1 chain A representing *Plasmodium falciparum* Plasmepsin I. This macromolecule has four chains (A, B, C, and D) figured out in Figure 3a. Receptor 3QS1 has two residues: GOL and KN-10006 [49]. Residue KN-10006 or (4R)-3-[(2S,3S)-3-{[(2,6-dimethyl phenoxy)acetyl]amino}-2-hydroxy-4-phenylbutanoyl]-N-[(1S,2R)-2-hydroxy-2,3-dihydro-1H-inden-1-yl]-5,5-dimethyl-1,3-thiazolidine-4-carboxamide is an inhibitor that has a large molecular mass with several nitrogen and sulfur atoms (Figure 1e). Observations on each 3QS1 chain showed that all the chain has an active site, and in this current project, the molecular docking process is represented only in chain A.

Molecular docking analysis of ligand (3) and 3QS1 chain A produced the best affinity energy at -7.7 Kcal/mol compared to ligand (2) and chloroquine (Table 2). The complex of malaria receptor (PDB

1YVB) and isothiocyanate compounds was reported to have better affinities than chloroquine [50], it is in line with the 3QS1-A and 8DSR-B complex. The complex pattern of 3QS1 chain A and compound (3) can be seen in the insert of Figure 4c, whereas the close-up 2D interactions and bonding 3D patterns were laid in Figure 4a and 4b, respectively. Since this current work uses *P. falciparum* 3D7 sensitive chloroquine for an *anti-Plasmodium* test, docking analysis of the chloroquine compound is used as a drug standard comparison. Compound (3) does not have a high similarity to the standard drug structure, however, each chloroquine and compound (3) has three nitrogen atoms that are assumed to play a significant binding in the receptor and ligand complex.

In the complex of 3QS1 chain A and ligand (3), there are 8 (eight) types of interactions, namely conventional hydrogen bonds on ASP32. Carbon Hydrogen bond interactions on LEU114, π – σ interactions on VAL76, Alkyl and π – alkyl interactions on VAL289, LEU291, PHE109A, ALA111, MET13, ILE30, PHE117, ILE120. Salt bridge and attractive charge on ASP215 and ASP32. Meanwhile, van der Waals interactions occur at ASP290, SER35, ILE300, TYR75, SER220, THR218, THR222, ILE287, GLY115, VAL12, SER219, SER77, GLY217, GLY34, and TYR189. All Plasmepsin I binding sites appear to play a role in the complex of 3QS1 chain A and compound (3), namely ILE30, TYR75, SER77, PHE109A, ILE120, GLY217, THR218, THR222, ILE300, SER219, ILE287 [49]. These include ASP32 and ASP215, which form salt bridges, attractive charge, and hydrogen bonds with three nitrogen-thiourea groups in the compound (3). Compared to complex 3QS1 chain A and chloroquine, there are 3 (three) types of interactions viz van der Waals, attractive charge, and alkyl interaction. Van der Waals on MET13, ILE30, ILE120, GLY217, SER77, THR218, THR222, VAL76, ILE300, GLY34, TYR75, PHE109A, ALA111 and PHE 117. However, ASP215 and ASP32 in 3QS1-A only interacted with one nitrogen-chloroquine by attractive charge (Figure 4d-4f). This indicates that molecule (3) is a potent *anti-plasmodial* compound through the food vacuole inhibition pathway, which will inhibit parasite growth in erythrocytes.

Molecular docking analysis was also carried out using a macromolecule with

PDB code 8DSR chain B, which represents *Plasmodium falciparum* Plasmepsin X (Figure 3b). Observation in this macromolecule reveals that 8DSR has two chains (A and B) and one KWU residue on each chain. KWU residue or (2E,6S)-6-{2-chloro-3-[(2-cyclopropylpyrimidin-5-yl)amino]phenyl}-2-imino-6-methyl-3-[(2S,4S)- 2-methyloxan-4-yl]-1,3-diazinan-4-one) is an inhibitor that has a relatively large molecular weight and contains several nitrogen and chlorine atoms (Figure 1f). Analysis of the molecular docking of ligand (3) and 8DSR chain B produces better affinity energy with a value of -7.6 Kcal/mol compared to ligand (2) and chloroquine, which have affinity energy of -6.5 Kcal/mol and -6.1 Kcal/mol, respectively (Table 2). The appearance complex of 8DSR chain B and compound (3) are presented in the insert of Figure 5c and zoomed-in as a 2D and 3D interaction pattern (Figure 5a-5b).

In the complex of 8DSR chain B and ligand (3), there are 8 (eight) types of interactions, namely van der Waals interactions, attractive charge, carbon-hydrogen bonds, conventional hydrogen bonds, π–σ interactions, π–alkyl, π–anion, and π–sulfur interactions. The 8DSR active site was located on ASP457, ASP266, and THR460 [28]. The observation results show that ASP 457 and ASP266 interact via attractive charge and π–anion interaction with one Nitrogen atom and aromatic in compound (3), while THR460 forms a conventional hydrogen bond with Oxygen - methoxy in the methyl eugenol group. In the complex of 8DSR chain B and chloroquine, there are 8 (eight) types of interaction viz van der Waals, attractive charge, conventional hydrogen bond, π-anion, π-sigma, π-π T-shape, alkyl and π-alkyl interactions. Only two of the 8DSR active residues were inside this complex. Direct interaction only occurs between ASP266 and one Nitrogen-chloroquine in an attractive charge and π-anion types. THR460 residue lies around the chloroquine as a van der Waals bond (Figure 5d-5f). This indicates that molecule (3) has the potential as an *anti-Plasmodium* compound through the maturase inhibition pathway for rhoptry and microneme proteins.

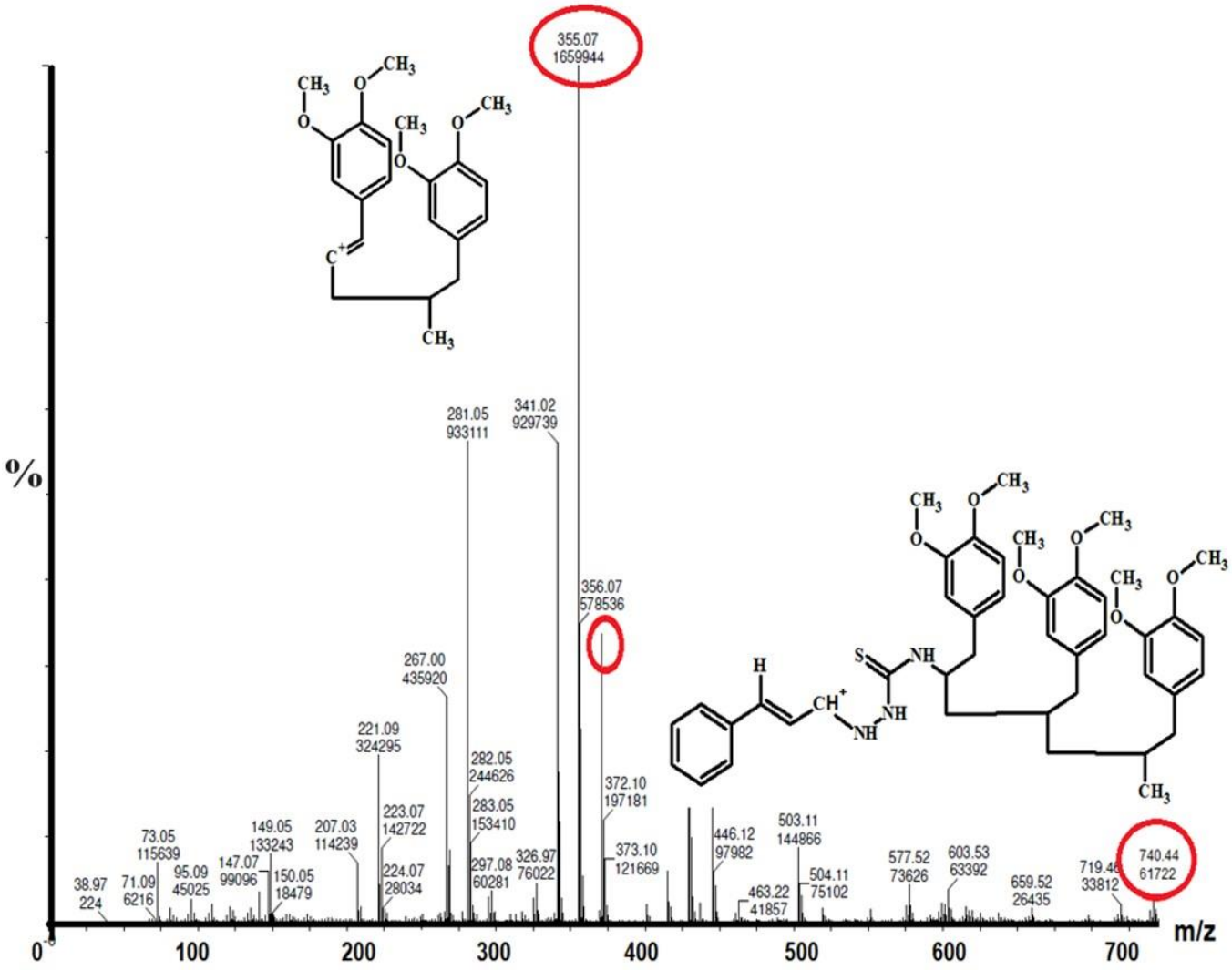

Figure 2. LCMS-MS spectrum of compound (3).

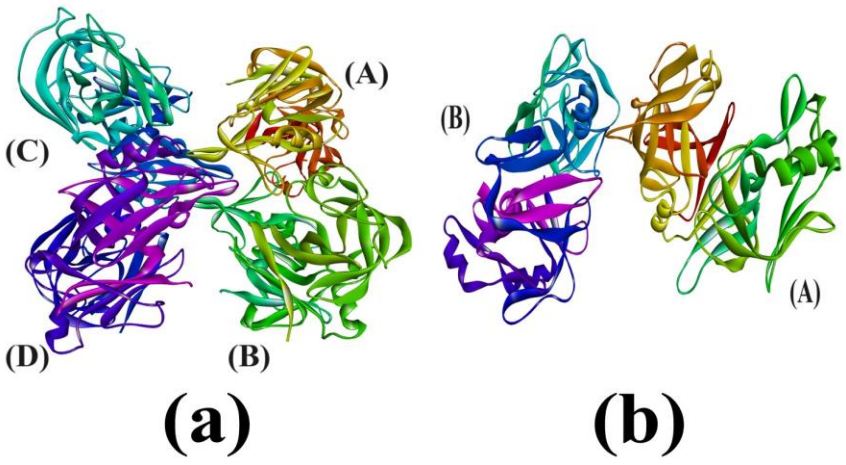

Figure 3. Plasmodium falciparum: (a). 3QS1, (b). 8DSR.

Table 2. Binding affinities

Complex:	Binding Affinity (Kcal/mol)
3QS1 chain A and chloroquine	-6.9
3QS1 chain A and compound (2)	-7.1
3QS1 chain A and compound (3)	-7.7
8DSR chain B and chloroquine	-6.1
8DSR chain B and compound (2)	-6.5
8DSR chain B and compound (3)	-7.6

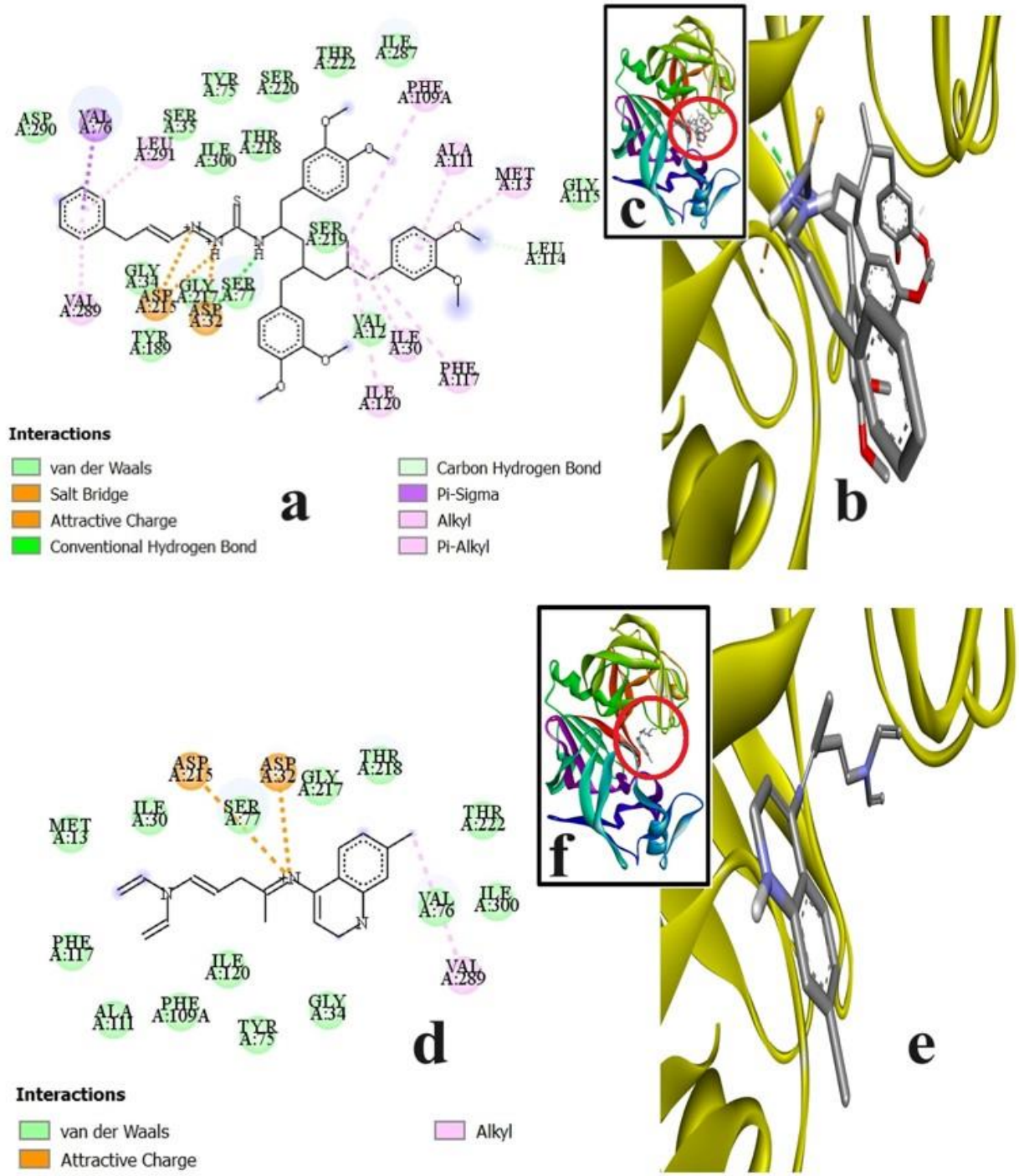

Figure 4. The zoomed-in view of 3QS1 chain A and ligand (3) in (a). 2D interactions, (b). 3D binding pose, (c). complex of 3QS1-A and ligand (3). A close-up view of 3QS1 chain A and chloroquine in (d). 2D interactions, (e). 3D binding pose, (f) complex of 3QS1-A and chloroquine.

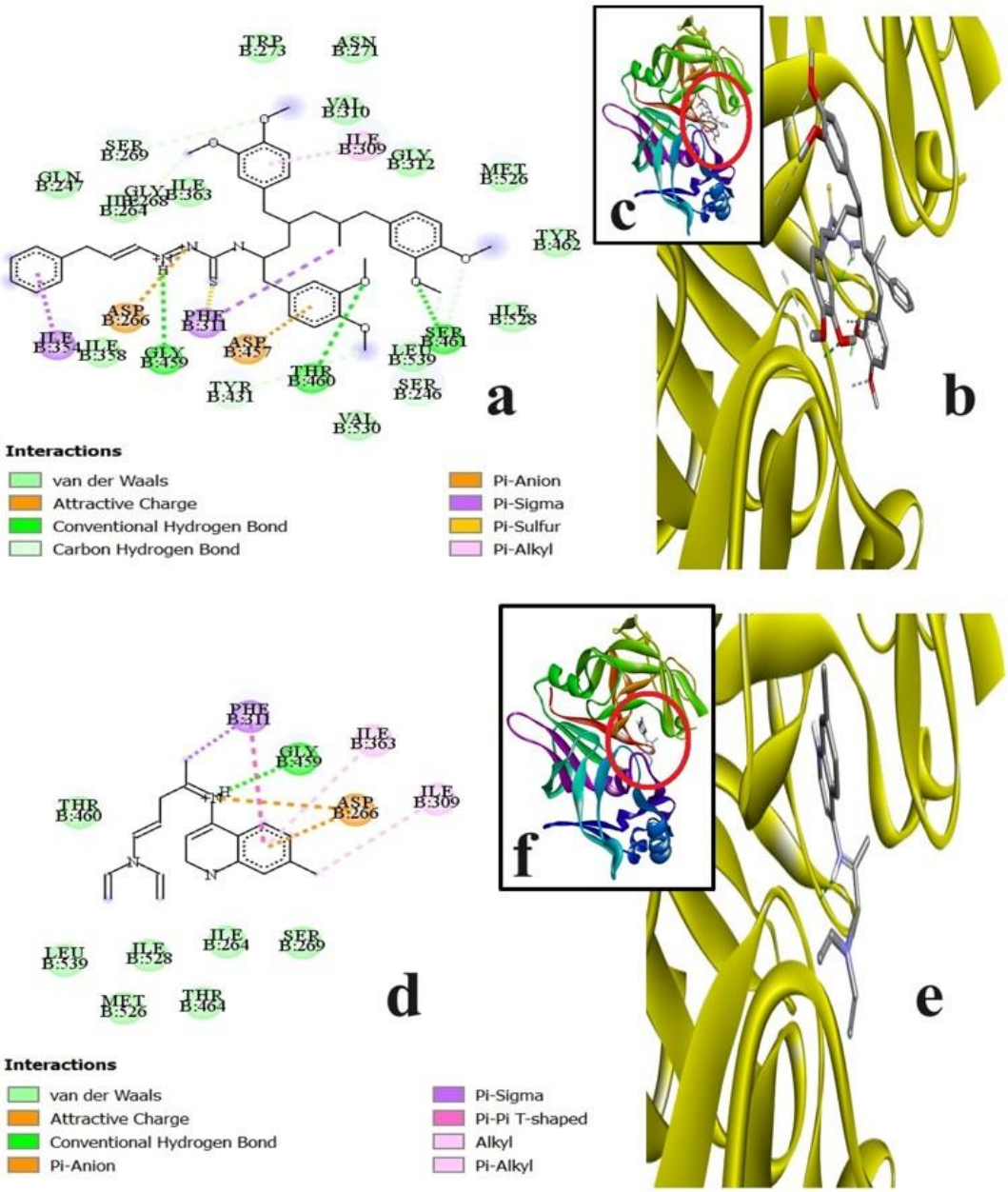

Figure 5. The zoomed-in view of 8DSR chain B and ligand (3) in (a). 2D interactions, (b). 3D binding pose, (c). complex of 8DSR-B and ligand (3). A close-up view of 8DSR chain B and chloroquine in (d). 2D interactions, (e). 3D binding pose, (f). complex of 8DSR-B and chloroquine.

DISCUSSION

Thiourea and urea have a similar structural framework (Figure 1d), with differences in the sulfur and oxygen atoms [51]. Thiourea compounds are generally synthesized by forming isothiocyanate compounds (N=C=S), although the thiocyanate compounds have the potential to form. The first stage reaction between isothiocyanate and hydrazine compounds will produce a thiosemicarbazide derivative, whereas the second stage reaction between thiosemicarbazide derivative compounds and compounds containing aldehyde groups will produce a thiosemicarbazone derivative. These two reaction stages can be reduced to one step using the one-pot reaction method to create a thiourea derivative known as the thiosemicarbazone compound [34].

In this current work, the synthesized thiourea derivatives by the first-stage reaction to MIE isothiocyanate (compound 1) and ME isothiocyanate (compound 2) was forming. However, because compound (1) has a thiocyanate wavenumber and gave a low yield, only compound (2) was used for the second-stage reaction. Cinnamaldehyde (Figure 1c) is used as the aldehyde compound provided. The one-pot reaction between compound (2), hydrazine, and cinnamaldehyde produces a thiosemicarbazone derivative compound (compound 3) that the structure proposed in Figure 2.

The synthesis of thiourea derivatives via the isothiocyanate synthesis route using ME as renewable starting materials has been successfully carried out. Synthesis product analysis and bioactivity tests support the use of this compound as a future *anti-Plasmodium* alternative. The difficulty of separating isothiocyanate precursor compounds can be overcome by forming thiourea derivatives for further purification processes. It is important to note that this compound has a high Molecular Weight (MW); therefore, synthesis reaction conditions are necessary to consider to prevent the polymerization process, and hopefully, a low molecular weight of thiourea derivative will be obtained.

CONCLUSION

The thiourea derivative (compound 3) based on methyl eugenol and cinnamaldehyde was synthesized using the one-pot reaction method. This method was carried out by forming a methyl eugenol isothiocyanate derivative compound (2).

The spectral analysis predicted that the product formed was the polymerization result of methyl eugenol cinnamaldehyde thiosemicarbazone. Compound (3) had active potency against *Plasmodium falciparum* 3D7. Molecular docking study through 2D and 3D observations got an insight that ligand (3) is an *anti-Plasmodium* compound through the food vacuole and the maturase inhibition pathways for rhoptry and microneme proteins.

ACKNOWLEDGMENT

It is part of doctoral thesis. All authors would like to thank the Universitas Brawijaya for partially funding this work through Hibah Guru Besar 2020-2021. Highly appreciation is also conveyed to Institut Atsiri - Universitas Brawijaya for research facilitation.

REFERENCES

[1]. Fajemiroye JO, Galdino PM, De Paula JAM, Rocha FF, Akanmu MA, Vanderlinde FA, *et al.* Anxiolytic and antidepressant like effects of natural food flavour (E)-methyl isoeugenol. *Food Funct.* 2014; 5(8): 1819–28.

[2]. Paula JAM, Ferri PH, Bara MTF, Tresvenzol LMF, Sá FAS, Paula JR. Infraspecific chemical variability in the essential oils of Pimenta pseudocaryophyllus (gomes) l.r. landrum (myrtaceae). *Biochem Syst Ecol.* 2011; 39(4–6): 643–50.

[3]. Nazlić M, Fredotović Ž, Vuko E, Vuletić N, Ljubenkov I, Kremer D, *et al.* Free volatile compounds of veronica austriaca ssp. jacquinii (baumg.) eb. fisch. and their biological activity. *Plants*. 2021; 10(11): 2529.

[4]. Silva S, Barata J, Lopes V, Barata A, Gomes A, Silva L, *et al*. Chemical composition of the essential oils in Portuguese daucus carota subspecies. KnE *Materials Sci.* 2022; 72–79.

[5]. Choudhury M, Ramakrishnan E, Devi D. Identification and characterization of methyl isoeugenol compound from the golden yellow hued muga silk fiber of India. *J Nat Fibers.* 2021; 18(8): 1069–82.

[6]. Bonilla-Castañeda SM, Villamizar-Mogotocoro AF, Kouznetsov VV. [4-(3,4-Dimethoxyphenyl)-3,6-dimethyl-2-phenyl-3,4-dihydroquinolin-1(2H)-yl)](furan-2-yl)methanone. *Molbank.* 2022(3): 1413.

[7]. Rodríguez Enciso DA, Puerto Galvis CE, Kouznetsov VV. 2-(4-Chlorophenyl)-

4-(3,4-dimethoxy-phenyl)-6-methoxy-3-methylquinoline. *Molbank*; 2022(2): 1383.

[8]. Rudyanto M, Hartanti L. One-step conversion of eugenol to methyl isoeugenol using microwave irradiation in solvent-free conditions. *Indones J Chem.* 2010; 6(3): 292–96.

[9]. Santana Ht, Trindade Ftt, Stabeli Rg, Silva Aae, Militão Jstl, Facundo Va. Essential oils of leaves of Piper species display larvicidal activity against the dengue vector, Aedes aegypti (Diptera: Culicidae). *Rev Bras Plantas Med.* 2015; 17(1): 104–11.

[10]. Eloh K, Kpegba K, Sasanelli N, Koumaglo H, Caboni P. Nematicidal activity of some essential plant oils from tropical West Africa. *Int J Pest Manage.* 2019; 66: 1–11.

[11]. Royer JE, Teakle GE, Ahoafi E, Mayer DG. Methyl-isoeugenol, a significantly more attractive male lure for the methyl eugenol-responsive Pacific fruit fly, *Bactrocera xanthodes* (Diptera: Tephritidae). *Austral Entomol*. 2019; 58(4): 800–4.

[12]. Agustian E, Tursiloadi S, Sulaswatty A, Rinaldi N, Sudiyarmanto. One-pot conversion and separation of methyl eugenol by vacuum fractionation. *IOP Conf Ser: Mater Sci Eng.* 2019; 494(012056): 1–7.

[13]. Barboza JN, Filho C da SMBF, Silva RO, Medeiros JVR, de Sousa DP. An overview on the anti-inflammatory potential and antioxidant profile of eugenol. *Oxid Med Cell Longevity.* 2018; 2018: 1–9.

[14]. Rathore N, Nizami T. Traditional herbal medicine in the treatment of patients infected with new Coronavirus. *Health Biotech Biopharm*. 2021; 4(4): 6–15.

[15]. Ke C, Liu Q, Li L, Chen J, Wang X, Huang K. Simultaneous determination of eugenol, isoeugenol and methyleugenol in fish fillet using gas chromatography coupled to tandem mass spectrometry. *J Chromatogr B: Anal Technol Biomed Life Sci*. 2016; 1031: 189–94.

[16]. Bakhs A, Hassan MW, Maqsood S, Sarwar G. Evaluation of methyl eugenol doses against bactrocera zonata s. (diptera: tephritidae) in ber fruit orchard in Bahawalpur, *Pakistan. BioSci Rev.* 2022; 4(3): 73–82.

[17]. Joshi A, Prakash O, Pant AK, Kumar R, Szczepaniak L, Kucharska-Ambrożej K. Methyl eugenol, 1,8-cineole and nerolidol

rich essential oils with their biological activities from three *melaleuca* species growing in tarai region of north India. *Braz Arch Biol Technol.* 2021; 64: 21210186.

[18]. Sanli A, Ok FZ. Chemical composition and antimicrobial activity against phytopathogenic fungi of essential oils obtained from Echinophora tenuifolia subsp. sibthorpiana grown in wild and cultivated conditions in Turkey. *Molecules.* 2023; 28(2): 585.

[19]. Medagedara HK, Paranagama PA, Gunaratna MJ. Detailed evaluation of methylated and acetylated products of cinnamon leaf oil against *Aedes aegypti*. *Proceeding of the 1st International Conference on Frontiers in Chemical Technology*. 2020: 56.

[20]. Qian Y, Zhang J, Yu Y, Jiang Q, Yan B, Song X, et al. Preparation of long-lasting releasing methyl eugenol fiber membrane and its trapping analysis on Bactrocera dorsalis. *Polymer*. 2023; 285: 126349.

[21]. Arianie L, Hermanto FE, Dhiaul Iftitah E, Warsito W, Widodo N. Novel antimalarial drug screening based on methyl eugenol, cinnamaldehyde, and thiosemicarbazone with cysteine protease inhibition: in silico molecular docking, molecular dynamics, and admet studies. *J Pure Appl Chem Res.* 2022; 11: 102–12.

[22]. Catalano A, Iacopetta D, Pellegrino M, Aquaro S, Franchini C, Sinicropi MS. Diarylureas: Repositioning from Antitumor to Antimicrobials or Multi-Target Agents against New Pandemics. *Antibiotics.* 2021; 10(1): 92.

[23]. Huizing AP, Mondal M, Hirsch AKH. Fighting malaria: structure-guided discovery of nonpeptidomimetic plasmepsin inhibitors: miniperspective. J Med Chem. 2015; 58(13): 5151–63.

[24]. Nasamu AS, Polino AJ, Istvan ES, Goldberg DE. Malaria parasite plasmepsins: More than just plain old degradative pepsins. *J Biol Chem.* 2020; 295(25): 8425–41.

[25]. Ishola AA, Adewole KE, Adebayo JO, Balogun EA. Potentials of terpenoids as inhibitors of multiple Plasmodium falciparum protein drug targets. *Acta Parasit*. 2023; 68(4): 793–806.

[26]. Mishra V, Rathore I, Arekar A, Sthanam LK, Bedi RK, Patel C, *et al*. Structure-based designing of inhibitors against plasmepsins from Plasmodium falciparum. Rochester, NY; 2020.

[27]. Hodder AN, Christensen J, Scally S, Triglia T, Ngo A, Birkinshaw RW, *et al.* Basis for drug selectivity of plasmepsin IX and X inhibition in Plasmodium falciparum and vivax. *Structure*. 2022; 30(7): 947-61.

[28]. Lowe MA, Cardenas A, Valentin JP, Zhu Z, Abendroth J, Castro JL, *et al*. Discovery and characterization of potent, efficacious, orally available antimalarial plasmepsin x inhibitors and preclinical safety assessment of ucb7362. *J Med Chem.* 2022; 65(20): 14121–43.

[29]. Nasamu AS, Glushakova S, Russo I, Vaupel B, Oksman A, Kim AS, *et al.* Plasmepsins IX and X are essential and druggable mediators of malaria parasite egress and invasion. *Sciences.* 2017; 358(518–522): 1–5.

[30]. Arianie L, Supriatna MI, Kazal N, Widodo N, Warsito W, Iftitah ED. Synthesis, in vitro, and in silico studies of methyl eugenol derivatives for Plasmodium falciparum inhibitor. *Trop J Nat Prod Res*. 2022; 6(9): 1446–54.

[31]. Arianie L, Supriatna MI, Kazal N, Widodo N, Warsito W, Iftitah ED. Synthesis and characterization of isothiocyanate poly(methyl eugenol) and thiosemicarbazide poly(methyl eugenol). *Mater Sci Forum.* 2022; 1074: 23–32.

[32]. Batista A SA, Vandresen F, Falzirolli H, Britta E, de Oliveira DN, Catharino RR, *et al*. Synthesis and comparison of antileishmanial and cytotoxic activities of S-(−)-Limonene benzaldehyde thiosemicarbazones with their R-(+)-Analogues. *J Mol Struct.* 2019; 1179: 252–62.

[33]. Bozgeyik E, Tasdemir-Kahraman D, Arman K, Bozgeyik I, Karakucuk-Iyidogan A, Cakmak EA. Novel thiosemicarbazone derivative 17b interferes with the cell cycle progression and induce apoptosis through modulating downstream signaling pathways. *Gene Rep*. 2020; 18: 100578.

[34]. Cunha S, da Silva TL. One-pot and catalyst-free synthesis of thiosemicarbazones via multicomponent coupling reactions. *Tetrahedron Lett*. 2009; 50(18): 2090–93.

[35]. Karaküçük-İyidoğan A, Aydınöz B, Taşkın-Tok T, Oruç-Emre EE, Balzarini J. Synthesis, biological evaluation and ligand based pharmacophore modeling of new aromatic thiosemicarbazones as potential anticancer agents. *Pharm Chem J*. 2019; 53(2): 139–49.

[36]. Vandresen F, Falzirolli H, Almeida Batista SA, da Silva-Giardini APB, de Oliveira DN, Catharino RR, et al. Novel r-(+)-limonene-based thiosemicarbazones and their antitumor activity against human tumor cell lines. *Eur J Med Chem. 2*014; 79: 110–16.

[37]. Xiabing M, Ablajan K, Obul M, Seydimemet M, Ruzi R, Wenbo L. Facial one-pot, three-component synthesis of thiazole compounds by the reactions of aldehyde/ketone, thiosemicarbazide and chlorinated carboxylic ester derivatives. *Tetrahedron*. 2016; 72(18): 2349–53.

[38]. Hidayati AR, Widyawaruyanti A, Ilmi H, Tanjung M, Widiandani T, Siswandono S S, et al. Antimalarial activity of flavonoid compound isolated from leaves of Artocarpus altilis. *Pharmacogn J.* 2020; 12(4): 835–42.

[39]. Hidayati AR, Melinda, Ilmi H, Sakura T, Sakaguchi M, Ohmori J, *et al.* Effect of geranylated dihydrochalcone from Artocarpus altilis leaves extract on Plasmodium falciparum ultrastructural changes and mitochondrial malate: Quinone oxidoreductase. *Int J Parasitol Drugs Drug Resist*. 2023; 21: 40–50.

[40]. Dallakyan S, Olson AJ. Small-molecule library screening by docking with PyRx. In: Hempel JE, Williams CH, Hong *Chemical Biology.Springer New York*; 2015; 243–50.

[41]. Eberhardt J, Santos-Martins D, Tillack AF, Forli S. Autodock vina 1.2.0: new docking methods, expanded force field, and python bindings. *J Chem Inf Model*. 2021; 61(8): 3891–98.

[42]. Trott O, Olson AJ. Autodock vina: improving the speed and accuracy of docking with a new scoring function, efficient optimization, and multithreading. *J Comput Chem.* 2009; 31(2): 455–61.

[43]. Anitha L, Saritha SR, Layana SR, Nair Lakshmi CS, Hubert Joe I, Sudarsanakumar MR. Structural studies of 3-[(e)-[(2e)-2-methyl-3-phenylprop-2-en-1-ylidene] amino]-1-phenylthiourea: combined experimental and computational studies. *J Mol Struct*. 2019; 1191: 206–17.

[44]. Sambandam S, Sarangapani B, Paramasivam S, Chinnaiyan R. Molecular structure, vibrational spectral investigations (ft-ir and ft-raman), nlo, nbo, homo-lumo, mep analysis of (e)-2-(3-pentyl-2,6-diphenylpiperidin-4-ylidene)-n-phenylhydrazinecarbothioamide based on

dft and molecular docking studies. *Biointerface Res Appl Chem.* 2020; 11(4): 11833–55.

[45]. Huseynova M, Farzaliyev V, Medjidov A, Aliyeva M, Özdemir M, Taslimi P, *et al.* Synthesis, biological and theoretical properties of crystal zinc complex with thiosemicarbazone of glyoxylic acid. *J Mol Struct.* 2022; 1248: 131470.

[46]. Kozyra P, Korga-Plewko A, Karczmarzyk Z, Hawrył A, Wysocki W, Człapski M, *et al.* Potential anticancer agents against melanoma cells based on an as-synthesized thiosemicarbazide derivative. *Biomolecules.* 2022; 12(2): 151.

[47]. Patel DB, Darji DG, Patel KR, Rajani DP, Rajani SD, Patel HD. Synthesis of novel quinoline-thiosemicarbazide hybrids and evaluation of their biological activities, molecular docking, molecular dynamics, pharmacophore model studies, and ADME-tox properties. *J Heterocyclic Chem.* 2020; 57(3): 1183–200.

[48]. Sardari S, Shahcheragh SM, Habibi A, Shirzad M, Farahani Y. One pot, green synthesis and biological evaluation of some isatin-based thiocarbohydrazones derivatives. *Health Biotech Biopharm.* 2023; 6(4): 81–97.

[49]. Bhaumik P, Horimoto Y, Xiao H, Miura T, Hidaka K, Kiso Y, *et al*. Crystal structures of the free and inhibited forms of plasmepsin I (PMI) from Plasmodium falciparum. *J Struct Biol.* 2011; 175(1): 73–84.

[50]. Arianie L, Widodo, Iftitah ED, Warsito. Natural isothiocyanate anti-malaria: molecular docking, physicochemical, ADME, toxicity and synthetic accessibility study of eugenol and cinnamaldehyde. *Int J App Pharm.* 2021; 13(6): 82–88.

[51]. Shakeel A. Thiourea derivatives in drug design and medicinal chemistry: a short review. *J drug des med chem.* 2016; 2(1): 10–20.